IEEE Access
Multidisciplinary | Rapid Review | Open Access Journal

Received June 6, 2019, accepted June 14, 2019, date of publication June 26, 2019, date of current version July 19, 2019.

Digital Object Identifier 10.1109/ACCESS.2019.2924918

Power Quality Disturbance Recognition Based on Multiresolution S-Transform and Decision Tree

TIE ZHONG[1,2], SHUO ZHANG[2], GUOWEI CAI[2], YUE LI[3], BAOJUN YANG[3], AND YUN CHEN[2]

[1]Key Laboratory of Modern Power System Simulation and Control and Renewable Energy Technology, Ministry of Education, Northeast Electric Power University, Jilin 132012, China
[2]Department of Electrical Engineering, Northeast Electric Power University, Jilin 132012, China
[3]Department of Information Engineering, Jilin University, Jilin 130012, China

Corresponding author: Yue Li (519647817@qq.com)

This work was supported in part by the China Postdoctoral Science Foundation under Grant 2018M631839, and in part by the Excellent Youth Foundation of Jilin Scientific Committee under Grant 20180520091JH.

ABSTRACT It is important to find an effective method for power quality (PQ) disturbance recognition under the challenges of increasing power system pollution. This paper proposes a PQ disturbance signal recognition method based on Multiresolution S transform (MST) and decision tree (DT). For improving recognition accuracy, adjustment factors are introduced to obtain a controllable time-frequency resolution. On this basis, five feature statistics are obtained to quantitatively reflect the characteristics of the analyzed power quality disturbance signals, which is less than the traditional S-transform-based method. As the proposed methodology can effectively identify the PQ disturbances, the efficiency of the DT classifier could be guaranteed. In addition, the noise impacts are also taken into consideration, and 16 types of noisy PQ signals with a signal-to-noise ratio (SNR) scoping from 30 to 50 dB are used as the analyzed dataset. Finally, a comparison between the proposed method and other popular recognition algorithms is conducted. The experimental results demonstrate that the proposed method is effective in terms of detection accuracy, especially for combined PQ disturbances.

INDEX TERMS Multiple power quality disturbances, multiresolution S-transform, feature extracting, disturbance classification, decision tree.

I. INTRODUCTION

Electric power has become an indispensable part of national life, and improving the PQ conditions has great significances in the normal operations for power grids. Recently, with the development of modern electronic technology, a large number of unbalanced non-linear loads and new energy with random fluctuation characteristics have been added to the power grids, resulting in many PQ disturbance events, such as harmonic and transient disturbances [1]–[3]. These disturbance events have negative impacts on the performances for the equipment based on precision computers and microprocessors, in some conditions, even bring some unexpected consequences [4]. Therefore, investigating PQ signals is of great significance in improving power supply quality, monitoring equipment state and troubleshooting.

The PQ disturbance contains a large amount of power system operation information [5], [6]. Through the analysis of time-frequency information, such as the evolution of the energy and frequency component, the fault location and type can be obtained, which provides important basis for the quick repair of power systems. Moreover, rapid advances in power technology have provided new ways to cope with the challenges facing smart management of power systems. PQ analysis also plays an important role in transient analysis and monitoring of power equipment [7]. At the same time, the increasing complexity of disturbance types also puts forward higher requirements for PQ disturbance recognition. Accurate and real-time identification of disturbance has attracted increasing attention in power industry.

In general, PQ disturbance recognition can be divided into several parts, such as disturbance signal detection, feature extraction, disturbance classification and recognition. Generally, the disturbance signals of PQ are non-stationary, and most of the disturbances in the power systems represent as the combination of several disturbances, which require high efficiency for the signal analysis methods. Common signal analysis methods including Kalman filtering (KF) [8],

The associate editor coordinating the review of this manuscript and approving it for publication was Zhixiang Zou.

short-time Fourier transform (STFT) [9], wavelet transform (WT) [10], discrete wavelet transform (DWT) [11], wavelet packet transform (WPT) [12], Hilbert-Huang transform (HHT) [13], multiple time-window spectrum estimation (MTW) [14], and S-transform (ST) [15]. By comparing with other method, the processing results for ST is excellent and the time-frequency resolution is relatively great, thus, for precise analysis signal properties, ST has become one of the most widely used methodologies [16]. However, it is known that the optimal resolutions for time and frequency cannot be obtained simultaneously [17], and this degrades the accuracy of the detection algorithm, especially for the combined disturbances analysis. Furthermore, recognition is another critical procedure, and common disturbance classification methods mainly including fuzzy expert system (FES) [8], support vector machine (SVM) [18], extreme learning machine (ELM) [19], artificial neural network (ANN) [20], probabilistic neural network (PNN) [11], K-nearest neighbor [21] and decision tree (DT) [14], etc. Unfortunately, traditional classification methods show some deficiencies when faced with complex and massive PQ data, such as ANN needs to be retrained when a new type of disturbances appears [22]. Compared to other approaches, DT is easier to construct, and its real-time processing capability is better than other methods although its classification accuracy depends on the selected features. If the features are clearly distinguishable from each other, then the efficiency of the DT method is excellent.

In this paper, a PQ disturbance recognition algorithm based on Multiresoltion-ST (MST) and DT is proposed. Here, MST [23], which is an improved algorithm of ST, uses parameters to adjust the window function to achieve a controllable time-frequency resolution. In addition, it has been used successfully in research on seismic signal processing. By applying the MST, the time-frequency characteristics of the analyzed PQ signals are investigated, while 5 feature statistics for each PQ signal are obtained. On this basis, DT classifier was used to classify the PQ signal according to the feature statistics. Due to the efficiency of MST, the efficiency for the DT classifier could be guaranteed. For checking the capability of the proposed algorithm, 16 types of PQ disturbance signals with SNRs of 30-50dB, 7 of them are combined PQ disturbances, are used as the dataset. In addition, the field PQ data is also investigated. The experimental results show that the proposed algorithm is efficient in detecting PQ disturbances with better accuracy, even under low SNR conditions.

The rest of the paper is organized as follows: In Section II, the theoretical background of the proposed PQ disturbance recognition algorithm is introduced. Section III gives the framework for the proposed PQ detection methodology. Section IV and Section V present the experiments to verify the efficiency of the proposed methodology in detecting and classifying PQ disturbances, especially for the field dataset. Finally, Section VI concludes the paper.

II. THE METHODS

A. S-TRANSFORM

The basic idea of ST is similar with STFT, while its window function feature changes with frequency, which overcomes the defects of the conventional algorithms. The time-frequency matrix contains adequate time-frequency information, and disturbance characteristics, such as amplitude and harmonic component, could be obtained.

In general, if the processing signal is $x(t)$, then its ST processing results $S(t,f)$ could be denoted as:

$$S(t,f) = \int_{-\infty}^{\infty} x(\tau) g(t-\tau, f) e^{-i2\pi f t} d\tau \tag{1}$$

$$g(t,f) = \frac{|f|}{\sqrt{2\pi}} e^{-\frac{t^2 f^2}{2}} \tag{2}$$

where, τ is a shift factor and $g(t,f)$ is a Gaussian window function with a width of $1/|f|$.

It can be found that the time-frequency resolution of the ST is closely related to the properties of the Gaussian window function. However, the window width is only determined by frequency in conventional ST, which means that the time-frequency resolution is fixed when the frequency is given [24]. Thus, conventional ST is difficult to meet the requirements when coping with complex combined disturbances in some conditions.

B. MULTIRESOLUTION S-TRANSFORM

In order to obtain a flexible time-frequency resolution, here, the adjustment factors for the window function, shown as parameters a, b and c in equation (3), have been introduced, while the width of the window function could be denoted as:

$$\sigma_f = \frac{1}{|af^b + c|} \tag{3}$$

It is shown that the width of the window function could be amended by changing the corresponding parameters, which is shown as follows:

$$g_1(t,f) = \frac{|af^b + c|}{\sqrt{2\pi}} e^{-\frac{t^2 (af^b + c)^2}{2}} \tag{4}$$

On this basis, the expression of MST can be described as:

$$S_{mst}(t,f) = \int_{-\infty}^{\infty} x(\tau) g_1(t-\tau, f) e^{-i2\pi f t} d\tau \tag{5}$$

As discussed above, the time-frequency resolution, which is related to window function characteristics, could be controlled by changing the window width factors. According to Heisenberg uncertainty principle, the time resolution and frequency resolution cannot reach the optimal at the same time. Therefore, the appropriate combination of parameters should be determined according to the actual situation of the PQ disturbance signal.

C. PARAMETERS DETERMINATION

For demonstrating the efficiency of the MST and investigating the parameter determination, a comparison is carried

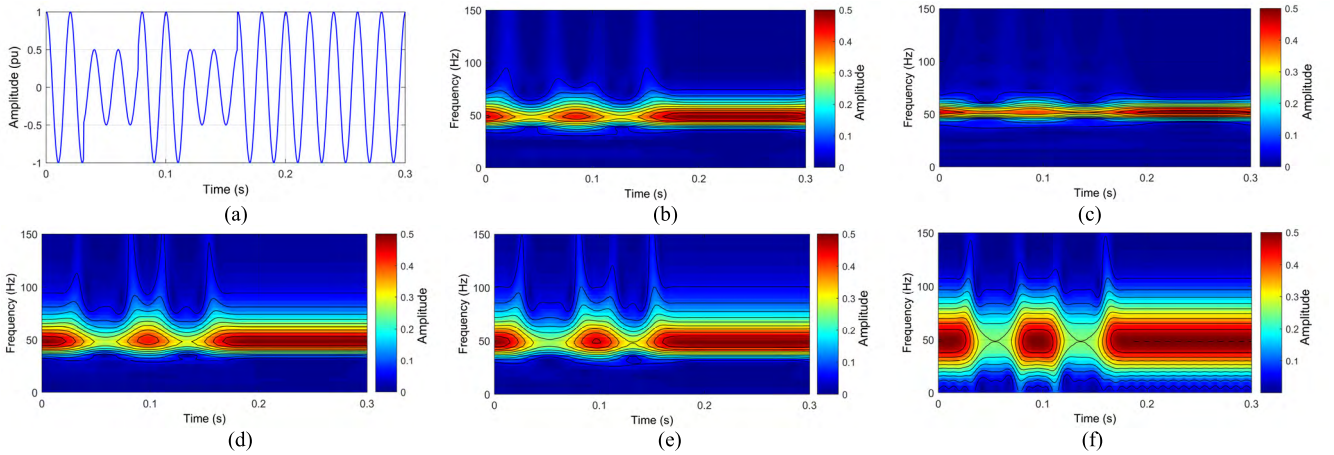

FIGURE 1. Time-frequency analyzing results for combined sag disturbance. (a) PQ waveform, (b) Standard ST, (c) Empirically selected window ST, (d) Double resolution ST, (e) Adaptive GW-based ST, and (f) MST used in this paper.

out with the following 4 versions of ST, including standard ST [15], empirically selected window ST [25], single parameter optimization-based ST [26] and adaptive Gaussian-window-based ST [27]. A multiple PQ disturbance signal, which has two voltage sag, are used as the test signal, while the waveforms is shown in Figure 1(a). Figure 1(b)-(e) depict the processing results of the comparing modified ST. It is observed that the competing algorithms are all failed to capture the time location of PQ events due to their high frequency resolution in low frequency band. In other words, the high frequency resolution could lead to high-energy concentration without considering the time localization of the signal. Furthermore, Figure 1(f) gives the result of the methodology used in this paper, with a parameter of a = 0.94, b = 0.81, and c = 16. By observing the figures, the used MST gives a better time localization of the PQ events and more time-frequency features are accurately reflected. As the experimental results show that the processing results of our method is superior to those of the other variants of ST in terms of reflecting features in PQ events.

It is known that PQ disturbance could be mainly divided into instantaneous and steady-state disturbance, while instantaneous disturbance refers to the disturbance signal mainly accidentally changes in amplitude features, such as swell and sag, then steady-state disturbance indicates the component for the disturbance signal is obviously degenerated, such as flicker and harmonic. Specifically, the characteristics for the flicker disturbance are always contained in low frequency, while those for sag, swell and interruption signals could be reflected by the fundamental frequency contents (50Hz or 60Hz). Besides, the harmonic and transient disturbance should be detected when analyzing frequency components between 100 to 700Hz and over 700Hz, respectively. From this viewpoint, different parameters should be applied for different frequency bands to extract the features for different PQ signals. In addition, we optimize the three parameters in MST using the energy concentration measure (ECM) approach in this study [28]. By optimizing the corresponding parameters, an optimal time-frequency representation could be obtained. However, due to the real-time requirement for the power systems, the computation cost for repeating the determination process for each PQ signal seems to be unacceptable. For solving this problem, we select fixed typical parameter sets to accomplish PQ signal analysis. Although the processing result maybe not the optimal, it still can reflect the properties for PQ signals. Hence, the frequency band are divided into low, medium and high frequency bands for the requirements of PQ signal detailed analysis, while the parameters are set to be [0.94 0.81 16], [1.04 1.17 36], and [0.91 0.82 16], respectively.

D. THE DESCRIPTION FOR THE DT CLASSIFIER

DT is a typical classification algorithm. Generally, the structure of DT is relatively simple, and less training data is required [14]. Compared with other classification algorithms, DT algorithm can accurately analyze large amount of data in a short time, thus it is competent to cope with mass data processing, which is one of the toughest challenges faced by modern smart grids. From the aforementioned illumination, if the effectiveness of the proposed detection algorithm is verified, thus the classification accuracy of the DT classifier could be guaranteed. Here, the structure of DT classifier and the decision rules are determined by the feature statistic distributions for PQ disturbances.

III. PROPOSED PQ DETECTION FRAMEWORK

In this section, a brief description for the PQ disturbance signals is given, including modeling equations and parameter scope. Moreover, the principle of the proposed PQ detection algorithm is introduced in detail.

A. THE MODELING FOR PQ DISTURBANCE SIGNAL

Here, 16 kinds of disturbance, 7 of which are combined disturbance, are generated. The PQ signal is simulated using MATLAB2015b, and its modeling equation and parameter range are shown in Table 1 [14]. Considering the noise influence in actual operation of power system, the signal with a SNR of 30-50dB is used as the analyzing dataset.

TABLE 1. PQ disturbance modeling signal equation and parameters.

Lable	Disturbance Class	Modeling Equations	Equations' Parameters
C1	Normal Signal	$h(t) = A\cos(\omega t)$	$A = 1(pu), f = 50Hz, \omega = 2\pi f, u(t) = \begin{cases} 1, t \geq 0 \\ 0, t < 0 \end{cases}$
C2	Sag	$h(t) = A\{1 - k(u(t-t_1) - u(t-t_2))\}\cos(\omega t)$	$0.1 < k < 0.9,\ 0.5T \leq t_2 - t_1 \leq 9T$
C3	Swell	$h(t) = A\{1 + k(u(t-t_1) - u(t-t_2))\}\cos(\omega t)$	$0.1 < k < 0.9,\ 0.5T \leq t_2 - t_1 \leq 9T$
C4	Interruption	$h(t) = A\{1 - k(u(t-t_1) - u(t-t_2))\}\cos(\omega t)$	$0.9 < k < 1,\ 0.5T \leq t_2 - t_1 \leq 9T$
C5	Flicker	$h(t) = A[1 + \alpha\cos(\beta\omega t)]\cos(\omega t)$	$0.1 \leq \alpha \leq 0.2,\quad 0.1 \leq \beta \leq 0.4$
C6	Transient	$h(t) = A\{\cos(\omega t) + k\exp[-(t-t_1)/\tau]\cos[\omega_n(t-t_1)]\}$	$0.1 < k < 0.8, 150 < 1/\tau < 1000$ $\omega_n = 2\pi f_n,\ 700\ Hz < f_n < 1600\ Hz$
C7	Harmonics	$h(t) = A\cos(\omega t) + \alpha_3\cos(3\omega t) + \alpha_5\cos(5\omega t) + \alpha_7\cos(7\omega t)$	$0.02 < \alpha_3 < 0.1, 0.02 < \alpha_5 < 0.1,\quad 0.02 < \alpha_7 < 0.1$
C8	Notch	$h(t) = A\cos(\omega t) - \mathrm{sgn}(\cos(\omega t)) \times \left\{\sum_{n=0}^{8} K[u(t-(t_1-0.02n)) - u(t-(t_2-0.02n))]\right\}$	$0.1 \leq K \leq 0.4$
C9	Spike	$h(t) = A\cos(\omega t) + \mathrm{sgn}(\cos(\omega t)) \times \left\{\sum_{n=0}^{8} K[u(t-(t_1-0.02n)) - u(t-(t_2-0.02n))]\right\}$	$0.1 \leq K \leq 0.4$
C10	Sag with Transient	$h(t) = A\{1 - k(u(t-t_1) - u(t-t_2))\}\cos(\omega t)$ $+A\ p\ \exp[-(t-t_3)/\tau]\cos[\omega_n(t-t_3)]$	$0.1 < k < 0.9, 0.5T \leq t_2 - t_1 \leq 9T, t_1 \leq t_3 \leq t_2$ $0.1 < p < 0.8, 150 < 1/\tau < 1000$ $\omega_n = 2\pi f_n,\ 700\ Hz < f_n < 1600\ Hz$
C11	Swell with Transient	$h(t) = A\{1 + k(u(t-t_1) - u(t-t_2))\}\cos(\omega t)$ $+A\ p\ \exp[-(t-t_3)/\tau]\cos[\omega_n(t-t_3)]$	$0.1 < k < 0.9, 0.5T \leq t_2 - t_1 \leq 9T, t_1 \leq t_3 \leq t_2$ $0.1 < p < 0.8, 150 < 1/\tau < 1000$ $\omega_n = 2\pi f_n,\ 700\ Hz < f_n < 1600\ Hz$
C12	Sag with Harmonic	$h(t) = A\{1 - k(u(t-t_1) - u(t-t_2))\}\cos(\omega t)$ $+\alpha_3\cos(3\omega t) + \alpha_5\cos(5\omega t) + \alpha_7\cos(7\omega t)$	$0.1 < k < 0.9, 0.5T \leq t_2 - t_1 \leq 9T,\quad 0.02 < \alpha_3 < 0.1$ $0.02 < \alpha_5 < 0.1, 0.02 < \alpha_7 < 0.1,$
C13	Interruption with Harmonic	$h(t) = A\{1 - k(u(t-t_1) - u(t-t_2))\}\cos(\omega t)$ $+\alpha_3\cos(3\omega t) + \alpha_5\cos(5\omega t) + \alpha_7\cos(7\omega t)$	$0.9 < k < 1, 0.5T \leq t_2 - t_1 \leq 9T,\quad 0.02 < \alpha_3 < 0.1$ $0.02 < \alpha_5 < 0.1, 0.02 < \alpha_7 < 0.1,$
C14	Swell with Harmonic	$h(t) = A\{1 + k(u(t-t_1) - u(t-t_2))\}\cos(\omega t)$ $+\alpha_3\cos(3\omega t) + \alpha_5\cos(5\omega t) + \alpha_7\cos(7\omega t)$	$0.9 < k < 1, 0.5T \leq t_2 - t_1 \leq 9T,\quad 0.02 < \alpha_3 < 0.1$ $0.02 < \alpha_5 < 0.1, 0.02 < \alpha_7 < 0.1,$
C15	Flicker with Harmonic	$h(t) = A[1 + \alpha\cos(\beta\omega t)]\cos(\omega t)$ $+\alpha_3\cos(3\omega t) + \alpha_5\cos(5\omega t) + \alpha_7\cos(7\omega t)$	$0.1 \leq \alpha \leq 0.2,\quad 0.1 \leq \beta \leq 0.4$ $0.02 < \alpha_3 < 0.1, 0.02 < \alpha_5 < 0.1,\quad 0.02 < \alpha_7 < 0.1$
C16	Transient with Harmonic	$h(t) = A\{\cos(\omega t) + k\exp[-(t-t_1)/\tau]\cos[\omega_n(t-t_1)]\}$ $+\alpha_3\cos(3\omega t) + \alpha_5\cos(5\omega t) + \alpha_7\cos(7\omega t)$	$0.1 < k < 0.8, 150 < 1/\tau < 1000$ $\omega_n = 2\pi f_n,\ 700\ Hz < f_n < 1600\ Hz$ $0.02 < \alpha_3 < 0.1, 0.02 < \alpha_5 < 0.1,\quad 0.02 < \alpha_7 < 0.1$

The sampling rate is set to be 3.2 kHz. By observing the Table 1, we can obtain that the combined PQ disturbance signals could be viewed as several single disturbance occurring simultaneously.

B. TIME-FREQUENCY ANALYSIS OF PQ SIGNAL

The two-dimensional matrix of MST contains a large amount of signal time-frequency information, while the characteristics for each PQ signal should be reflected by its energy and frequency features. To extract the time-frequency information of the signal effectively, fundamental frequency contents $J(t)$, local power $P(t)$ and local frequency $F(t)$ are calculated, and definition is shown as follows:

$$\begin{aligned} J(t) &= S_{mst}(t, 50Hz); \\ P(t) &= \int_0^{\infty} S_{mst}(t,f)df; \\ F(t) &= \frac{1}{P(t)}\int_0^{\infty} f^3 \cdot S_{mst}(t,f)df \end{aligned} \tag{6}$$

where $S_{mst}(t, f)$ is the time-frequency matrix of MST. By observing the equation, we can get the point that $J(t)$ reflects the energy distribution in fundamental frequency. Similarly, $P(t)$ represents the evolvement trend of the signal energy, while $F(t)$ represents the similar contents with regard of frequency components.

Here, 8 types of single disturbance signals are analyzed by applying MST, and the results are shown in Figure 2. In each figure, the 4 subfigures, from top to bottom, depict the waveform, foundational frequency (50Hz or 60 Hz) contents, local power and local frequency curves. By observing the figures, the foundation frequency contents and local power for sag, swell and interruption signal have the similar evolvement trend with its waveform, while those for flicker signal fluctuates periodically. Moreover, the local power for harmonic signal are dominated by high-frequency fluctuations, whereas the local frequency contents for transient signal represents as large-amplitude increment when signal occurring. Thus, we can conclude that the properties for

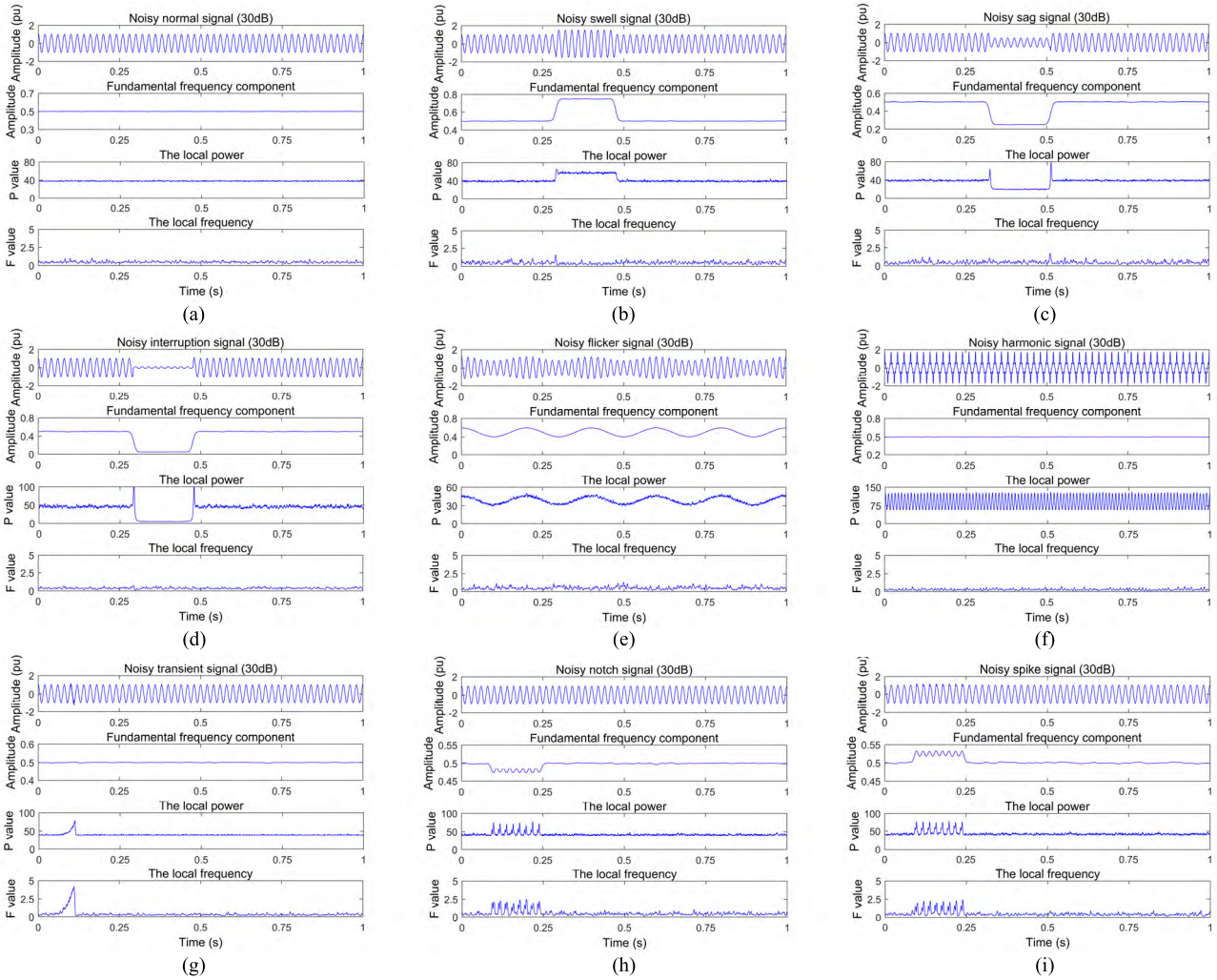

FIGURE 2. Comparisons between eight kinds of signal disturbances. (a) The normal signal, (b) The swell disturbance, (c) The sag disturbance, (d) The interruption disturbance, (e) The flicker disturbance, (f) The harmonic disturbance, (g) The transient disturbance, (h) The notch disturbance, and (i) The spike disturbance.

single disturbance could be effectively reflected based on the proposed algorithm.

Furthermore, the combined disturbance processing results are given in Figure 3. It is shown that the characteristics for single disturbance, shown in Figure 2, could still be observed, such as the combined disturbance with a sag or swell signal exhibit a clear trend with respect to local power. From this viewpoint, the combined disturbance, which are seen as the combination of single disturbances, could be detected, and the results represent that the combined disturbances are distinguishable in their energy and frequency properties. In summary, the experimental results verify that the time-frequency characteristics for the PQ disturbance signals could be effectively reflected by the proposed methodology, while it provides a reliable basis for the corresponding signal recognition.

C. FEATURE STATISTICS FOR DETECTION

Through the aforementioned discuss, the characteristics for PQ disturbance could be effectively reflected through fundamental frequency components, local power and local frequency contents. For achieving disturbance intelligent recognition, the features for PQ signals should be quantitatively represented, thus five statistics are proposed based on PQ event characteristics. Here, the description for the feature statistics are given as follows:

Feature 1 and 2 (The Maximum and Minimum Amplitudes of the Fundamental Frequency Components $A_{\max}$ and $A_{\min}$):

The maximum and minimum amplitudes at the fundamental frequency (50Hz or 60Hz) are defined as the first two feature statistics, and the definition are shown below:

$$A_{\max} = \frac{\max[G(p)]}{G_0}; A_{\min} = \frac{\min[G(p)]}{G_0} \tag{7}$$

where $G(p)$ and G_0 denotes the mean of the fundamental frequency contents for the PQ disturbances and standard signal. Specifically, $G(p)$ could be acquired by the following

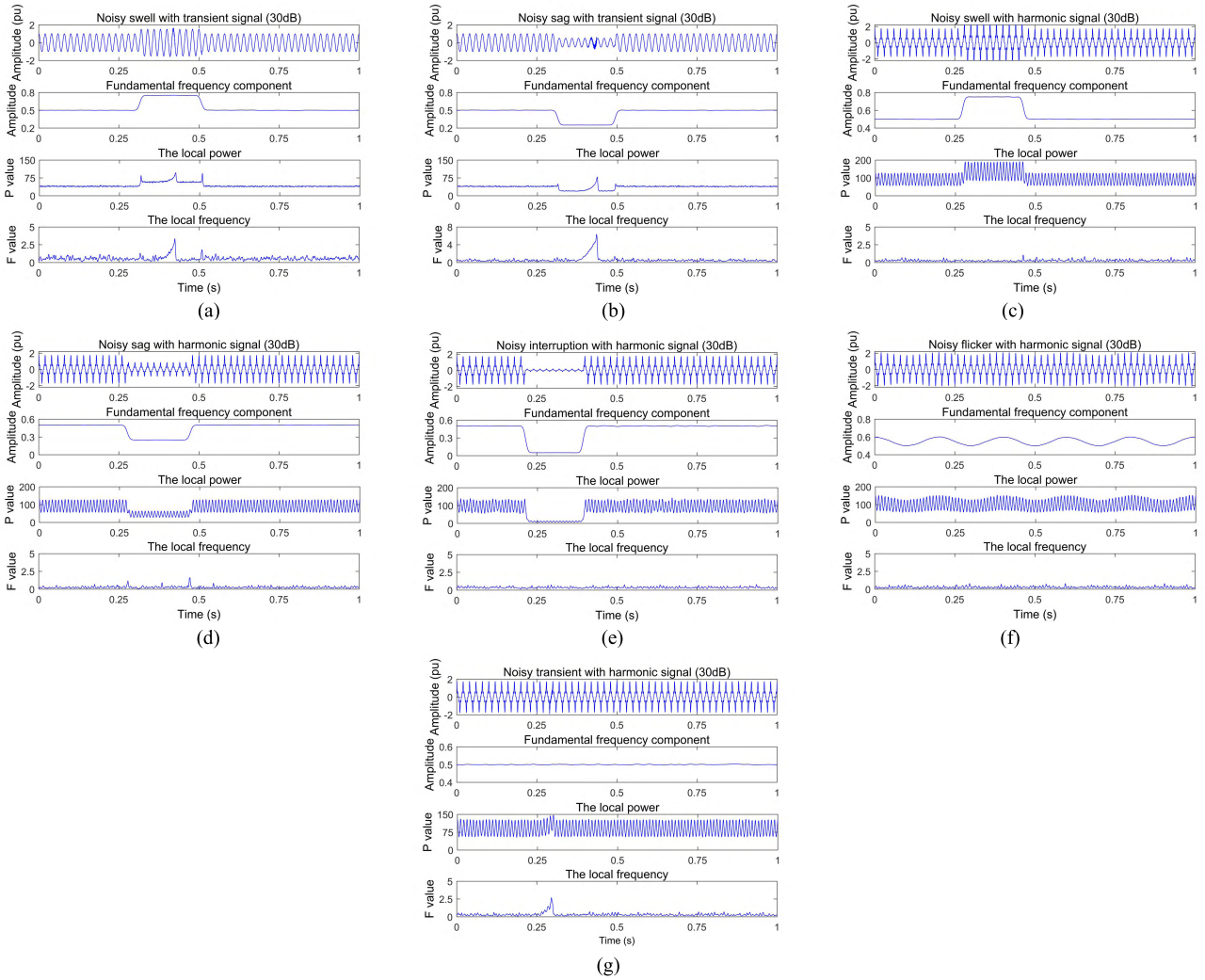

FIGURE 3. Comparisons between seven kinds of combined disturbances. (a) The swell with transient disturbance, (b) The sag with transient disturbance, (c) The swell with harmonic disturbance, (d) The sag with harmonic disturbance, (e) The interruption with transient disturbance, (f) The flicker with harmonic disturbance, and (g) The transient with harmonic disturbance.

equation.

$$G(p) = \frac{1}{N} \sum_{t_p=1+(p-1)N}^{pN} J(t_p) \tag{8}$$

where $J(t_p)$ indicates the fundamental frequency curves around time position t_p, while N is set be 50 in this study. Feature 1 and 2 investigate the evolvement trend for the fundamental frequency components. The characteristics for the PQ signals, whose energy distribution exhibits a clear trend such as swell and sag, could be accurately described by these two features.

Feature 3 (The Correlation Coefficient for Fundamental Frequency Components Sb):

The aforementioned experimental results, shown in Figure 2 and 3, indicate that the periodical fluctuation fashion is a significant feature to detect flicker events. In addition, flicker events with different amplitude scopes have similar fluctuation characteristics. Thus, the flicker events should be effectively recognized by checking if an obvious periodical fluctuation existing. On this basis, the correlation coefficient with fundamental frequency components for flicker events is proposed as the Feature 3, while the definition equation is shown as follows:

$$S_b = \frac{Cov[J(t), J_0(t)]}{\sqrt{Var[J(t)] \cdot Var[J_0(t)]}} \tag{9}$$

where $J(t)$ and $J_0(t)$ denotes the fundamental frequency components for the analyzed signal and flicker disturbances, respectively.

Feature 4 (The Harmonic Energy Ratio for the Local Power K_p):

It is shown that the local power for harmonic events represent as high-frequency vibrations. By applying multitaper algorithm [29], the power spectrum density (PSD) of local power for flicker, harmonic disturbance and flicker with

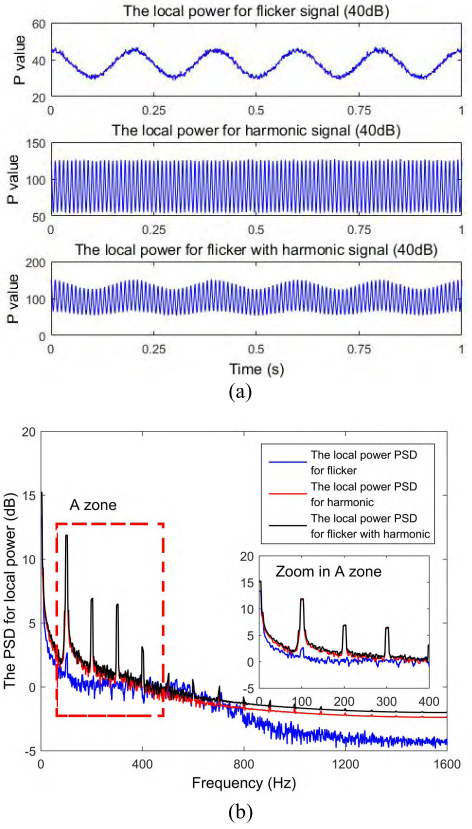

FIGURE 4. Comparisons the PSD for local power between flicker, harmonic, and flicker with harmonic disturbances. (a) The local power comparison, and (b) The PSD comparision.

harmonic disturbance are compared in Figure 4. It is shown that harmonic components are easy to be observed in PSD for PQ disturbances with harmonic, thus the harmonic energy ratio in local power are used as the Feature 4. Here, the K_p is defined below:

$$K_p = \frac{\int_{95}^{105} M(f)df}{\int_0^{\infty} M(f)df};$$
$$M(f) = \frac{1}{K}\sum_{k=1}^{K}\left|\int_0^{\infty} P(t)\cdot d_K(t)\cdot \exp(-2\pi ft)dt\right|^2 \quad (10)$$

where $M(f)$ represents the PSD for analyzed PQ disturbance estimated by multitaper algorithm, which is superior to the FFT method in terms of estimated bias and frequency resolution. Moreover, $P(t)$ denotes the local power for PQ signal, whereas $d_K(t)$ and K represent the orthogonal window function and the number of window functions, respectively.

Feature 5 The Maximum Value for the Local Frequency K_f):

As aforementioned, the local frequency contents for the transient signal represents as large-amplitude increasement when signal occurring. Thus, it could be used as the criteria for the transient events recognition, and the maximum value for the local frequency contents, denotes as K_f, is used as the Feature 5.

$$K_f = \frac{\max[F_1(p)]}{F_0} \quad F_1(p) = \frac{1}{N}\sum_{t_p=1+(p-1)N}^{pN} F(t_p) \quad (11)$$

where $F_1(p)$ and F_0 denotes the mean of the local frequency contents for the PQ disturbances and standard signal, respectively.

In order to verify the effectiveness of the feature statistics, the processing results for sag and swell signal is used as an example, and the comparison results are shown in Figure 5. Figure 5(a) and (b) display the waveform, fundamental frequency component, local power and local frequency contents for the PQ signal from the top to the bottom, while the comparisons between the feature statistics are shown in Figure 5(c). By analyzing the figures, it is noticed that the sag and swell disturbances could be distinguished by quantitatively comparing the Feature 1 and 2. Hence, we can get the point that the design for the proposed feature statistics is appropriate.

IV. EXPERIMENTATION AND RESULTS

For checking the capability of the proposed methodology, 16 types of PQ signals, 7 of them are combined disturbances, are processed. In the consideration of robustness, noisy disturbance signals, with a SNR ranging from 30 to 50dB, are used as the analysis dataset. Specifically, 2000 signals are generated for each kind of PQ disturbance according to the corresponding equation shown in Table 1. On this basis, 1000 signals are used to train the DT classifier, whereas others are used to check the accuracy of the DT classification results.

A. INVESTIGATION ON NOISE INFLUENCES

For checking the robustness, noisy flicker with harmonic signals, which have SNRs of 10dB, 20dB and 30dB shown in Figure 6(a)-(c), are investigated. By observing the figures, the periodical fluctuations in fundamental frequency contents, which are used to detect PQ disturbance with flicker events, are conspicuous enough to be observed, although that for the noisy signal with 10dB has some distortions due to the influence of strong interferences. Furthermore, the feature statistics for all the noisy signals are analyzed, the comparison results are depicted in Figure 6 (d), whereas the results indicate that the statistics for noisy PQ signals do not display an obvious deviation in terms of value distributions. Specifically, the statistics S_b for noisy events, used as the most significant criteria for flicker events, are 0.998, 0.991 and 0.929, respectively. In other words, we can deduce that the feature statistics has a relatively stable distribution range. Thus, we can confirm that the proposed method can extract the essential characteristics of PQ disturbances even under low SNR conditions.

B. THE FEATURE STATISTIC DISTRIBUTIONS FOR PQ DISTURBANCES

It is shown that the local energy and local frequency can directly reflect the condition of energy varies with frequency,

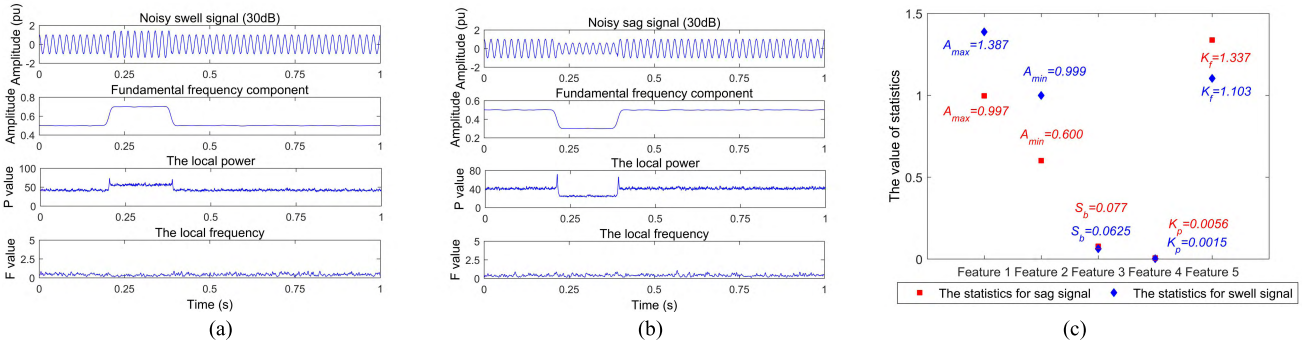

FIGURE 5. Comparisons of the swell and sag disturbance. (a) The results for the swell disturbance, (b) The results for the sag disturbance, and (c) The comparisons in feature statistics.

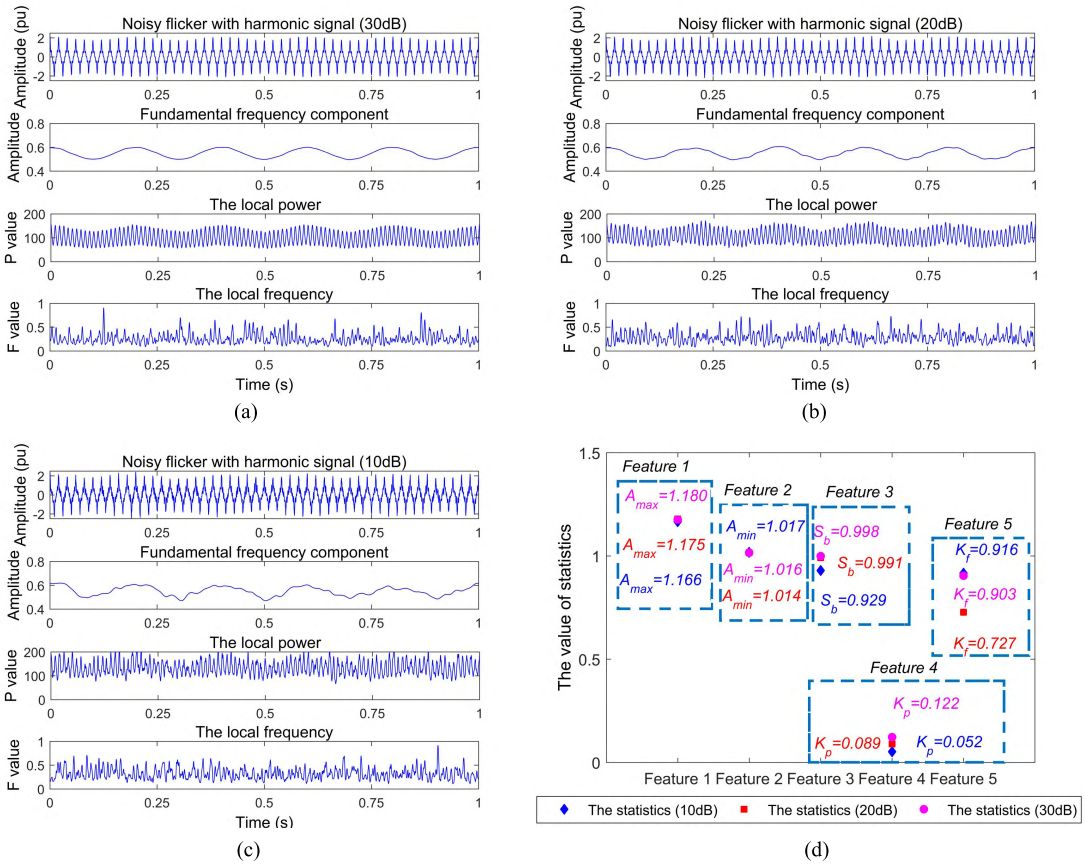

FIGURE 6. Robustness of the proposed method on detecting the noisy PQ signals. (a) Results for noisy PQ signal (30dB), (b) Results for noisy PQ signal (20dB), (c) Results for noisy PQ signal (10dB), and (d) Feature statistics distribution comparisons.

providing an important basis for the identification of combined disturbances. As aforementioned, 5 statistics for each PQ signal are calculated, and the analysis results are shown in Figure 7. Figure 7(a)-(b) give the evolution for statistics A_{max} and A_{min} obtained with different PQ signals. By observing the figures, it is shown that the disturbances with voltage sag and swell could be detected due to their temporary increasing or falling characteristics in fundamental frequency curves. Moreover, the contents shown in Figure 7(c) demonstrate that the PQ disturbance with harmonic could be perfectly recognized by comparing the statistics K_p. As aforementioned, the local power for harmonic events exhibits a clear high-frequency fluctuated fashion. From this viewpoint, the excellent effectiveness for the statistics K_p is reasonable. Similarly, as the results depicted in Figure 7(d)-(e), the PQ disturbance contained flicker or transient events could be

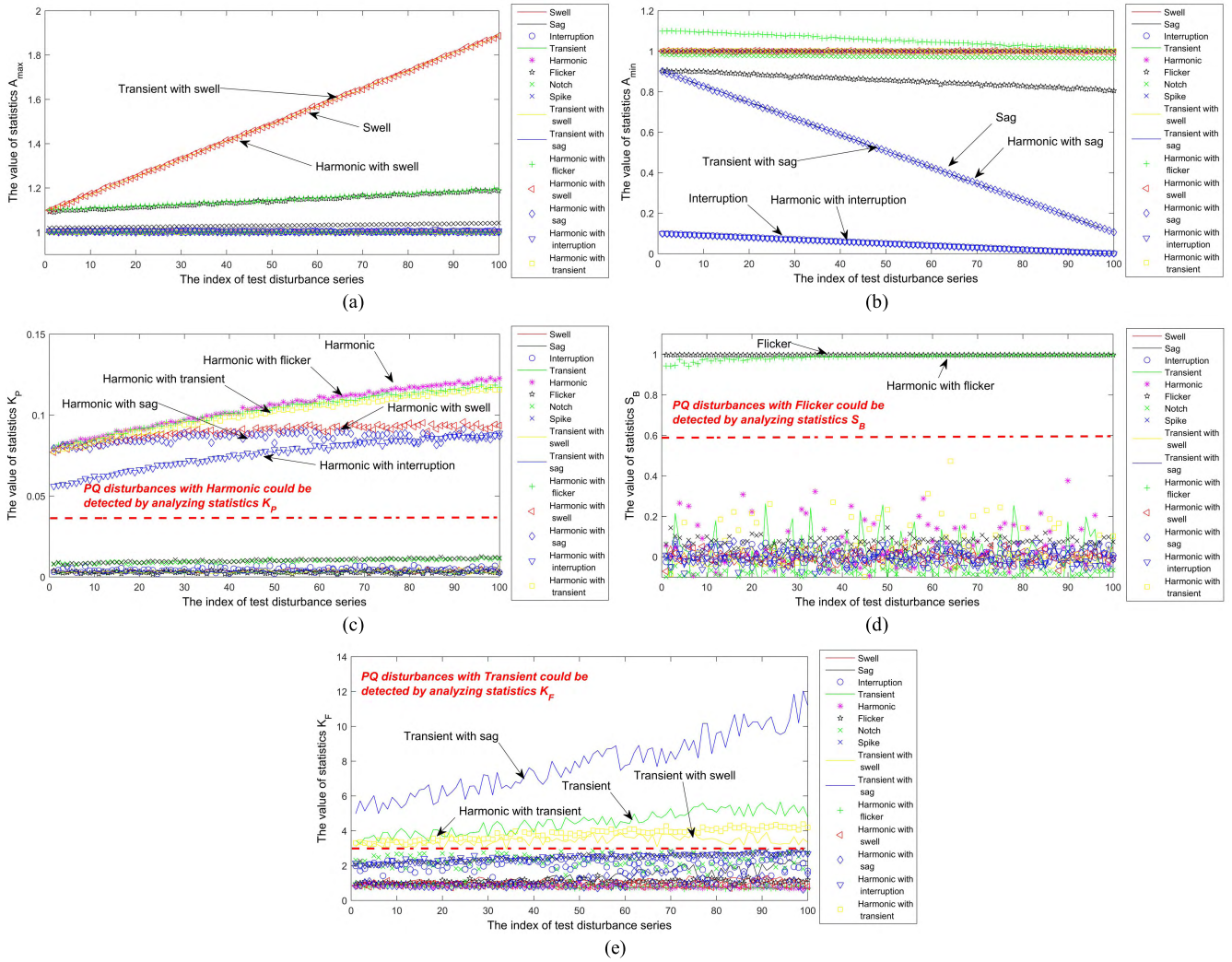

FIGURE 7. Feature statistic comparisons for the 12 kinds PQ disturbances. (a) A_{max} distributions for PQ signals, (b) A_{min} distributions for PQ signals, (c) K_p distributions for PQ signals, and (d) S_b distributions for PQ signals, and (e) K_f distributions for PQ signals.

captured by comparing statistics S_b and K_f, respectively. In summary, the experimental results indicate that the proposed feature statistics is efficient, while the characteristics for different PQ disturbances could be quantitatively reflected by them. Thus, the accuracy for DT classifier is guaranteed.

C. THE STRUCTURE OF DT CLASSIFIER

Given the aforementioned results, the efficiency of the feature-extracting algorithm is excellent. It means that the classification accuracy for DT classifier could be guaranteed. Hence, the decision rules for the DT classifier are constructed based on feature statistic distributions, and the corresponding contents are shown in Table 2. Here, "&&" means that the conditions should be satisfied simultaneously. For instance, if the statistics $0.8 \leq S_b \leq 1$ and $K_f \leq 2.9$, then the signal should be identified as flicker disturbance. Moreover, by analyzing the contents shown in Table 2 , it can be inferred that the DT classifier should have a 5-layer structure, and the PQ disturbances can be accurately recognized.

D. THE ANALYSIS OF RECOGNITION ACCURACY

To verify the accuracy of the proposed method, different PQ signals with a SNR of [30-50dB] is used as the analyzing dataset, while 2000 signals are generated for each type of disturbance. In addition, the recognition results are shown in Table 3. By observing the table, we can obtain that the accuracy slightly degrades with the SNR decreasing. However, the recognition accuracies are all above 97%, such as the flicker disturbances could be perfectly detected even under 30dB condition. Furthermore, we also compared our method with other popular recognition algorithms in terms of accuracy, number of selected features, and types of analyzed PQ signals. Specifically, Table 4 gives a detailed comparison with other 9 existing methods, while "–" denote that the corresponding conditions are not analyzed in the given algorithm.

TABLE 2. Decision rules for classification.

Label	Disturbance	Decision Rules for Classification
C1	Normal Signal	$(1 \le A_{max} \le 1.1) \&\& (0.9 \le A_{min} \le 1) \&\& (S_b \le 0.8) \&\& (K_p \le 0.05) \&\& (K_f \le 1.5)$
C2	Sag	$(0.1 \le A_{min} \le 0.9) \&\& (S_b \le 0.8) \&\& (K_p \le 0.05) \&\& (K_f \le 2.9)$
C3	Swell	$(1.1 \le A_{max} \le 1.9) \&\& (S_b \le 0.8) \&\& (K_p \le 0.05) \&\& (K_f \le 2.9)$
C4	Interruption	$(0.001 \le A_{min} \le 0.1) \&\& (S_b \le 0.8) \&\& (K_p \le 0.05) \&\& (K_f \le 2.9)$
C5	Flicker	$(0.8 \le S_b \le 1) \&\& (K_f \le 2.9)$
C6	Transient	$(1 \le A_{max} \le 1.1) \&\& (0.9 \le A_{min} \le 1) \&\& (S_b \le 0.8) \&\& (K_p \le 0.05) \&\& (K_f \ge 2.9)$
C7	Harmonics	$(1 \le A_{max} \le 1.1) \&\& (0.9 \le A_{min} \le 1) \&\& (S_b \le 0.8) \&\& (K_p \ge 0.05) \&\& (K_f \le 2.9)$
C8	Notch	$(1 \le A_{max} \le 1.01) \&\& (0.9 \le A_{min} \le 1) \&\& (S_b \le 0.8) \&\& (K_p \le 0.05) \&\& (1.6 \le K_f \le 2.6)$
C9	Spike	$(1 \le A_{max} \le 1.1) \&\& (0.99 \le A_{min} \le 1) \&\& (S_b \le 0.8) \&\& (K_p \le 0.05) \&\& (1.6 \le K_f \le 2.6)$
C10	Sag with Transient	$(0.1 \le A_{min} \le 0.9) \&\& (S_b \le 0.8) \&\& (K_p \le 0.05) \&\& (K_f \ge 2.9)$
C11	Swell with Transient	$(1.1 \le A_{max} \le 1.9) \&\& (S_b \le 0.8) \&\& (K_p \le 0.05) \&\& (K_f \ge 2.9)$
C12	Sag with Harmonic	$(0.1 \le A_{min} \le 0.9) \&\& (S_b \le 0.8) \&\& (K_p \ge 0.05) \&\& (K_f \le 2.9)$
C13	Interruption with Harmonic	$(0.001 \le A_{min} \le 0.1) \&\& (S_b \le 0.8) \&\& (K_p \ge 0.05) \&\& (K_f \le 2.9)$
C14	Swell with Harmonic	$(1.1 \le A_{max} \le 1.9) \&\& (S_b \le 0.8) \&\& (K_p \ge 0.05) \&\& (K_f \le 2.9)$
C15	Flicker with Harmonic	$(0.8 \le S_b \le 1) \&\& (K_p \ge 0.05)$
C16	Transient with Harmonic	$(1 \le A_{max} \le 1.1) \&\& (0.9 \le A_{min} \le 1) \&\& (S_b \le 0.8) \&\& (K_p \ge 0.05) \&\& (K_f \ge 2.9)$

TABLE 3. Recognition accuracy of the proposed method.

Types of disturbances	Accuracy of proposed method with dataset in different SNR (%)			
	Pure	50dB	40dB	30dB
Normal	100	100	100	99.9
Sag	99.9	99.8	99.5	99.3
Swell	100	100	99.7	99.5
Interruption	99.9	99.7	99.5	99.3
Flicker	100	100	100	100
Transient	100	99.9	99.1	98.2
Harmonics	100	100	100	100
North	100	99.7	99.3	98.7
Spike	100	99.8	99.5	98.9
Sag with Transient	100	100	99.5	98.1
Swell with Transient	100	100	99.7	98.3
Sag with Harmonic	99.9	99.7	99.7	98.9
Swell with Harmonic	100	100	100	100
Interruption with Harmonic	99.8	100	99.9	99.2
Flicker with Harmonic	100	100	100	100
Transient with Harmonic	100	100	99.7	97.0
AVE	**99.97**	**99.91**	**99.69**	**99.08**

TABLE 4. Comparison of classification accuracy with the existing methods.

Method Names	Number of features	Types of PQ signals	Accuracy of proposed method with dataset in different SNR (%)		
			Pure	40dB	30dB
KF and FES [8]	–	7	–	98.71	97
FFT and ANNS [30]	–	8	–	93.95	95.65
WT and PSO-ELM [19]	6	10	97.6	–	–
WPT and SVM [12]	15	8	98.3	–	–
DWT and PNN [11]	9	16	99.87	98.6	95.2
ST and PNN [22]	4	11	97.4	–	–
ST and Dynamics [31]	5	12	–	99.27	97.91
MGST and DT [32]	6	14	–	97.45	95.25
MTW and DT [14]	4	13	99.9	–	–
Proposed method	**5**	**16**	**99.97**	**99.69**	**99.08**

The competing algorithms include classical recognition algorithm, such as KF and FES [8], and recent proposed method, such as MTW and DT [14]. Due to similarity in analyzed dataset, we directly cited the recognition results published in the corresponding studies, and compared them with the results obtained by our method.

It is shown that the classification accuracy corresponding to the proposed algorithm is almost higher than all the other algorithms, especially under high-noise conditions (30dB). Thus, we can get the point safely that the comparing algorithms are all have their own deficiencies when coping with PQ signals with low SNRs. In summary, all the aforementioned experimental results suggest that the accuracy for the PQ recognition algorithm is excellent.

E. THE COMPUTATIONAL TIME COMPARISON

For investigating the computational time, 2000 PQ signals (3200-sample-long) are generated and used as the analyzed dataset. We select some common used algorithm as the competing methods to investigate the computational cost of the proposed method. Different algorithms are applied to the same dataset, and the mean computational time is used as the assessment criteria. Here, the experimental environment is composed by MATLAB2015b with a CPU (Intel i9-9900K, 3.6GHz) and 16G RAM. As shown in Figure 8,

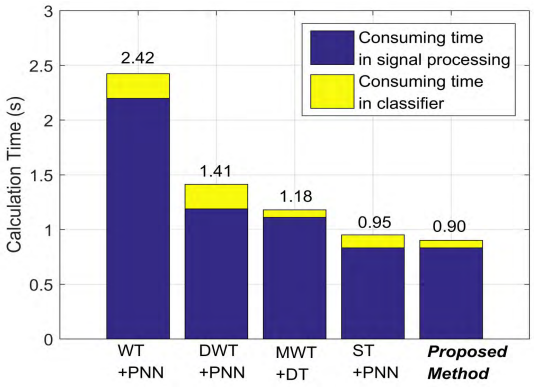

FIGURE 8. The computational time comparison.

the consuming time for our method is similar with recognition method based on ST and PNN, and less than other competing methodologies. It means that the computational cost for MST is similar with ST; however, the proposed method is significantly superior to it in terms of efficiency. In addition, the processing time could be further improved by investigating the corresponding fast calculation algorithm. In summary, the PQ disturbance could be detected by our method with less computational cost. All the aforementioned experimental results suggest that the proposed method has better real-time property, and it may satisfy the mass data processing requirement in modern smart grids.

V. FIELD PQ DISTURBANCE DATA PROCESSING RESULTS

For checking the efficiency of the proposed algorithm, the recognition accuracy for laboratory generated data and field PQ disturbance signals, captured in the actual grid, is also investigated. In laboratory environment, the signal source (Lecroy wave station 2052) is used to generate different PQ signals, whereas the oscilloscope (Lecroy wave runner 604 Zi), having recording function, is used to display and save the corresponding signals. Figure 9 (a) depicts the connection of the laboratory data acquisition system, while Figure 9 (b) gives a flicker signal, with modulation frequency 20Hz and modulation amplitude 0.2 pu, generated by the signal source. Moreover, field PQ disturbances are captured using the energy analysis equipment (Fluke 435 series II), which has been installed at a substation in campus, as illustrated in Figure 10. Here, 952 field PQ disturbances are recorded. The laboratory data and field data processing results are shown in Figure 11, while the waveform, fundamental frequency component, local power and local frequency are shown from top to bottom, respectively. Figure 11 (a) gives the processing results for a PQ signal generated in the laboratory environment, whereas Figure 11 (b) depicts the corresponding results for a field PQ disturbance. In Figure 11(a), it is noticed that a clear periodical fluctuation existing in the fundamental frequency, which is the most critical feature for recognizing flicker disturbance, whereas a diminutions have emerged in the amplitudes of the fundamental frequency and local power

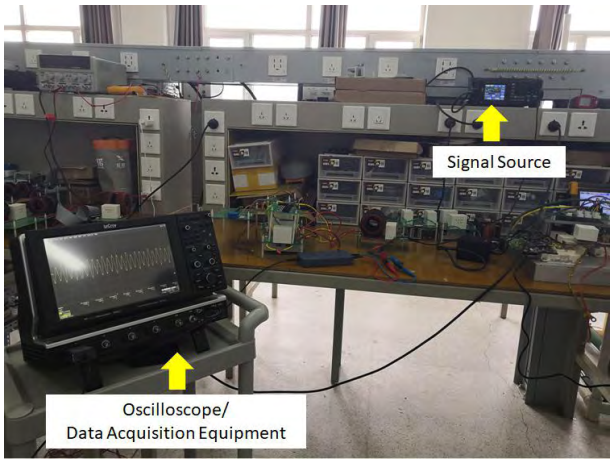

(a)

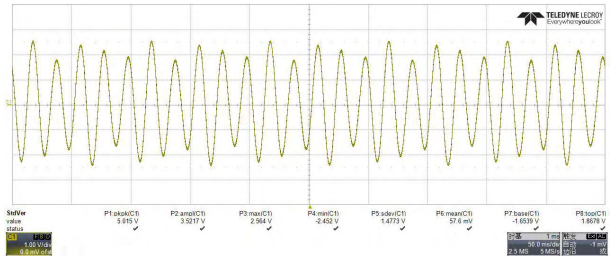

(b)

FIGURE 9. The composition for the PQ signals generating and recording system. (a) the connection of the system, and (b) the acquired flicker PQ disturbance.

FIGURE 10. The field data acquired condition at campus substation.

contents, shown in Figure 11 (b), which suggest that a sag disturbance has occurred. The statistic S_b for the PQ signals shown in Figure 11 (a) is 0.989 and K_f equals 1.212, which indicates that the signal should be classified as flicker disturbances. Moreover, the statistics A_{min} is 0.305, while K_P, K_F and S_b are all below the corresponding threshold, which denotes that the field signal is sag disturbance. The experimental results demonstrate that the proposed methodology

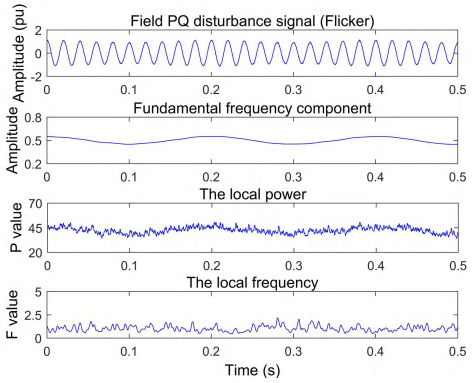

(a)

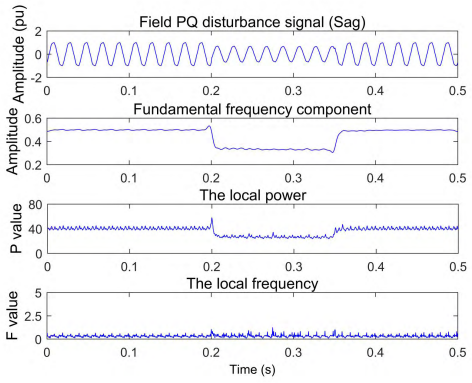

(b)

FIGURE 11. The processing results for the field PQ data. (a) The results for the flicker disturbance, and (b) The results for the sag disturbance.

could accurately detect the PQ event and track the voltage signal magnitude.

VI. CONCLUSION

In this paper, a PQ disturbance recognition method based on the MST and DT is proposed. We use adjustment factors to control the window function feature and amend the resolution for the time-frequency analyzing methods. For effectively extracting the disturbance characteristics, the frequency domain is divided into low, medium and high frequency bands, whereas the corresponding factors are determined respectively. On this basis, feature statistics are calculated, which could quantitatively reflect the PQ-signal properties, then DT classifier is constructed to accomplish the accurate recognition of the disturbances. We make a comparison with the other popular recognition algorithms, as the content shown in Table 4 , and the influence of noise is also taken into consideration. Noisy disturbance signals with a SNR ranging from 30dB to 50dB are used as the analyzing dataset. The experimental results demonstrate that the capability of the proposed methodology is excellent in recognition accuracy, such as the detection accuracy for the proposed methodology is 99.08% in 30dB condition, superior to all competing algorithms. In addition, only 5 feature statistics is needed, to our knowledge, which is less than most of the other popular methods, and the computational cost is relatively small. Furthermore, all these findings illuminate the effectiveness and accuracy of the proposed method. In summary, the proposed method is efficient in distinguishing PQ disturbances, especially for combined PQ disturbances. It has implications for conquering the challenges faced in modern smart grids.

ACKNOWLEDGMENT

(Tie Zhong and Guowei Cai contributed equally to this work.)

REFERENCES

[1] T. Yalcin and M. Ozdemir, "Pattern recognition method for identifying smart grid power quality disturbance," in *Proc. Int. Conf. Harmon. Qual. Power*, Belo Horizonte, Brazil, Oct. 2016, pp. 903–907.

[2] L. Peretto, M. Artioli, G. Pasini, and R. Sasdelli, "Performance analysis and optimization of a robust algorithm for voltage transients detection," *IEEE Trans. Instrum. Meas.*, vol. 55, no. 6, pp. 2244–2252, Dec. 2006.

[3] X. Shi, H. Yang, Z. Xu, X. Zhang, and M. R. Farahani, "An independent component analysis classification for complex power quality disturbances with sparse auto encoder features," *IEEE Access*, vol. 7, pp. 20961–20966, 2019.

[4] S. A. Kiranmai and A. J. Laxmi, "Data mining for classification of power quality problems using WEKA and the effect of attributes on classification accuracy," *Protection Control Mod. Power Syst.*, vol. 3, no. 1, p. 29, Jan. 2018.

[5] S. Khokhar, A. A. B. M. Zin, A. S. B. Mokhtar, and M. Pesaran, "A comprehensive overview on signal processing and artificial intelligence techniques applications in classification of power quality disturbances," *Renew. Sustain. Energy Rev.*, vol. 51, pp. 1650–1663, Nov. 2015.

[6] G. T. Heydt, P. S. Fjeld, C. C. Liu, D. Pierce, L. Tu, and G. Hensley, "Applications of the windowed fft to electric power quality assessment," *IEEE Trans. Power Del.*, vol. 14, no. 4, pp. 1411–1416, Oct. 1999.

[7] M. K. Saini and R. Kapoor, "Classification of power quality events—A review," *Int. J. Elect. Power Energy Syst.*, vol. 43, no. 1, pp. 11–19, Dec. 2012.

[8] A. A. Abdelsalam, A. A. Eldesouky, and A. A. Sallam, "Characterization of power quality disturbances using hybrid technique of linear Kalman filter and fuzzy-expert system," *Electr. Power Syst. Res.*, vol. 83, no. 1, pp. 41–50, Feb. 2012.

[9] J. Xu, Y. Zhang, Y. Li, and Y. Fan, "Comparative study of STFT and S transform on detecting voltage sag," *Power Syst. Protection Control*, vol. 42, no. 24, pp. 44–48, Dec. 2014.

[10] M. A. S. Masoum, S. Jamali, and N. Ghaffarzadeh, "Detection and classification of power quality disturbances using discrete wavelet transform and wavelet networks," *IET Sci., Meas. Technol.*, vol. 4, no. 4, pp. 193–205, Jul. 2010.

[11] S. Khokhar, A. A. M. Zin, A. P. Memon, and A. S. Mokhtar, "A new optimal feature selection algorithm for classification of power quality disturbances using discrete wavelet transform and probabilistic neural network," *Measurement*, vol. 95, pp. 246–259, Jan. 2017.

[12] K. Manimala, K. Selvi, and R. Ahila, "Optimization techniques for improving power quality data mining using wavelet packet based support vector machine," *Neurocomputing*, vol. 77, pp. 36–47, Feb. 2012.

[13] M. J. Afroni, D. Sutanto, and D. Stirling, "Analysis of nonstationary power-quality waveforms using iterative Hilbert Huang transform and SAX algorithm," *IEEE Trans. Power Del.*, vol. 28, no. 4, pp. 2134–2144, Oct. 2013.

[14] T. Zhong, S. Zhang, G. Cai, and N. Huang, "Power-quality disturbance recognition based on time-frequency analysis and decision tree," *IET Gener., Transmiss. Distrib.*, vol. 12, no. 18, pp. 4153–4162, Oct. 2018.

[15] R. G. Stockwell, L. Mansinha, and R. P. Lowe, "Localization of the complex spectrum: The S transform," *IEEE Trans. Signal Process.*, vol. 44, no. 4, pp. 998–1001, Apr. 1996.

[16] M. Meena, O. P. Mahela, M. Kumar, and N. Kumar, "Detection and classification of complex power quality disturbances using Stockwell transform and rule based decision tree," in *Proc. Int. Conf. Smart Electr. Drives Power Syst.*, Nagpur, India, Jun. 2018, pp. 220–226.

[17] N. C. F. Tse, J. Y. C. Chan, W.-H. Lau, and L. L. Lai, "Hybrid wavelet and Hilbert transform with frequency-shifting decomposition for power quality analysis," *IEEE Trans. Instrum. Meas.*, vol. 61, no. 12, pp. 3225–3233, Dec. 2012.

[18] P. Janik and T. Lobos, "Automated classification of power-quality disturbances using SVM and RBF networks," *IEEE Trans. Power Del.*, vol. 21, no. 3, pp. 1663–1669, Jul. 2006.
[19] R. Ahila, V. Sadasivam, and K. Manimala, "An integrated PSO for parameter determination and feature selection of ELM and its application in classification of power system disturbances," *Appl. Soft Comput.*, vol. 32, pp. 23–37, Jul. 2015.
[20] R. Kumar, B. Singh, D. T. Shahani, A. Chandra, and K. Al-Haddad, "Recognition of power-quality disturbances using S-transform-based ANN classifier and rule-based decision tree," *IEEE Trans. Ind. Appl.*, vol. 51, no. 2, pp. 1249–1258, Mar./Apr. 2015.
[21] B. K. Panigrahi and V. R. Pandi, "Optimal feature selection for classification of power quality disturbances using wavelet packet-based fuzzy k-nearest neighbour algorithm," *IET Gener., Transmiss. Distrib.*, vol. 3, no. 3, pp. 296–306, Mar. 2009.
[22] S. Mishra, C. N. Bhende, and B. K. Panigrahi, "Detection and classification of power quality disturbances using S-transform and probabilistic neural network," *IEEE Trans. Power Del.*, vol. 23, no. 1, pp. 280–287, Jan. 2007.
[23] N. Liu, J. Gao, B. Zhang, F. Li, and Q. Wang, "Time–frequency analysis of seismic data using a three parameters S transform," *IEEE Geosci. Remote Sens. Lett.*, vol. 15, no. 1, pp. 142–146, Jan. 2018.
[24] J. Li, Z. Teng, Q. Tang, and J. Song, "Detection and classification of power quality disturbances using double resolution S-transform and DAG-SVMs," *IEEE Trans. Instrum. Meas.*, vol. 65, no. 10, pp. 2302–2312, Oct. 2016.
[25] S. Assous and B. Boashash, "Evaluation of the modified S-transform for time-frequency synchrony analysis and source localisation," *EURASIP J. Adv. Signal Process.*, vol. 1, p. 49, Dec. 2012.
[26] E. Sejdic, I. Djurovic, and J. Jiang, "A Window Width Optimized S-transform," *EURASIP J. Adv. Signal Process.*, vol. 1, Dec. 2007, Art. no. 59.
[27] M. Biswal and P. K. Dash, "Estimation of time-varying power quality indices with an adaptive window-based fast generalised S-transform," *IET Sci., Meas. Technol.*, vol. 6, no. 4, pp. 189–197, Jul. 2012.
[28] A. Moukadem, Z. Bouguila, D. O. Abdeslam, and A. Dieterlen, "A new optimized Stockwell transform applied on synthetic and real non-stationary signals," *Digit. Signal Process.*, vol. 46, pp. 226–238, Nov. 2015.
[29] D. J. Thomson, "Spectrum estimation and harmonic analysis," *Proc. IEEE*, vol. 70, no. 9, pp. 1055–1096, Sep. 1982.
[30] F. A. S. Borges, R. A. S. Fernandes, I. N. Silva, and C. B. S. Silva, "Feature extraction and power quality disturbances classification using smart meters signals," *IEEE Trans. Ind. Informat.*, vol. 12, no. 2, pp. 824–833, Apr. 2016.
[31] S. He, K. Li, and M. Zhang, "A real-time power quality disturbances classification using hybrid method based on S-transform and dynamics," *IEEE Trans. Instrum. Meas.*, vol. 62, no. 9, pp. 2465–2475, Sep. 2013.
[32] N. Huang, S. Zhang, G. Cai, and D. Xu, "Power quality disturbances recognition based on a multiresolution generalized S-Transform and a PSO-improved decision tree," *Energies*, vol. 8, no. 1, pp. 549–572, Jan. 2015.

TIE ZHONG received the B.S., M.S., and Ph.D. degrees in communication engineering from Jilin University, Jilin, China, in 2016. He is currently an Associate Professor with the Communication Engineering Department, Northeast Electric Power University. He has published over 20 articles. His research interests include modern signal processing techniques, weak signal process theory, and intelligent information processing.

SHUO ZHANG was born in Qiqihar, Heilongjiang, China, in 1993. She received the B.S. degree in electronic information engineering from Northeast Electric Power University, Jilin, China, where she is currently pursuing the M.S. degree with the Communication Engineering Department. Her research interests include power quality disturbance analysis and signal processing.

GUOWEI CAI received the B.S. and M.S. degrees from Northeast Electric Power University, China, in 1990 and 1993, respectively, and the Ph.D. degree from the Harbin Institute of Technology, Harbin, China, in 1999. He is currently a Professor of electrical engineering with Northeast Electric Power University, Jilin, China. His research interests include power system stability analysis and control, and smart grid with renewable power generation.

YUE LI received the B.S. degree in automatic control from the University of Technology, Changchun, China, in 1982, and the Ph.D. degree in earthscope from Jilin University, Changchun, in 2001, where she is currently a Professor of communication and information system with the Department of Communication Engineering. She has authored over 100 papers on weak signal detection, real-time signal processing, nonlinear dynamic systems, random signal processing, Radon-Wigner transform, particle filter, and time-frequency analysis. She has coauthored two books, namely the *Methodology of Periodic Oscillator Detection* and the *Periodic Oscillator System and Detection*.

BAOJUN YANG received the B.S. degree from the Beijing Petroleum Institute, Beijing, China, in 1968, and the M.S. degree from the Changchun Geological Institute, Changchun, in 1981.

He was a Doctoral Supervisor with Jilin University, Changchun, where he enjoyed the government subsidy. From 1980 to 2008, he held various researches and teaching positions on seismic prospecting with Jilin University. He has coauthored 10 monographs and a series of textbooks. His research interests include the comprehensive information of lithosphere, the evaluation of oil-gas resource and petroleum exploration, and the nonlinear behavior of the seismic wave field.

Dr. Yang was a recipient of the first prize in scientific and technological progress from China's higher institution and the prize of science and technology outcome from the Ministry of Geology and Mineral Resources many times.

YUN CHEN was born in Baoding, Hebei, China, in 1997. She is currently pursuing the B.S. degree with the Communication Engineering Department, Northeast Electric Power University, Jilin, China. Her research interests include signal processing and machine learning.